Edinburgh Research Explorer

Factor associated with neutral sphingomyelinase activity mediates navigational capacity of leukocytes responding to wounds and infection

Factor Associated with Neutral Sphingomyelinase Activity Mediates Navigational Capacity of Leukocytes Responding to Wounds and Infection: Live Imaging Studies in Zebrafish Larvae

Alexandra Boecke,*[,1] Dirk Sieger,[†,1] Cristian Dan Neacsu,[‡] Hamid Kashkar,*[,§,¶] and Martin Krönke*[,§,¶]

Factor associated with neutral sphingomyelinase activity (FAN) is an adaptor protein that specifically binds to the p55 receptor for TNF (TNF-RI). Our previous investigations demonstrated that FAN plays a role in TNF-induced actin reorganization by connecting the plasma membrane with actin cytoskeleton, suggesting that FAN may impact on cellular motility in response to TNF and in the context of immune inflammatory conditions. In this study, we used the translucent zebrafish larvae for in vivo analysis of leukocyte migration after morpholino knockdown of FAN. FAN-deficient zebrafish leukocytes were impaired in their migration toward tail fin wounds, leading to a reduced number of cells reaching the wound. Furthermore, FAN-deficient leukocytes show an impaired response to bacterial infections, suggesting that FAN is generally required for the directed chemotactic response of immune cells independent of the nature of the stimulus. Cell-tracking analysis up to 3 h after injury revealed that the reduced number of leukocytes is not due to a reduction in random motility or speed of movement. Leukocytes from FAN-deficient embryos protrude pseudopodia in all directions instead of having one clear leading edge. Our results suggest that FAN-deficient leukocytes exhibit an impaired navigational capacity, leading to a disrupted chemotactic response. *The Journal of Immunology*, 2012, 189: 1559–1566.

T umor necrosis factor is a pleiotropic proinflammatory cytokine that specifically binds to the cell surface receptors TNF-RI (CD120a) and TNF-RII (CD120b). TNF-RI is bound with a higher affinity than TNF-RII, and most of the signaling pathways and subsequent biological effects are triggered by binding to TNF-RI (1, 2). TNF-RI is involved in many diverse cellular processes such as cell survival, proliferation, apoptosis, and inflammatory responses mediated by the activation of kinases of the MAPK family, transcription factors like NF-κB, and caspases. The activation of different signaling cascades is mediated by the different adaptor proteins that bind to the intracellular domains of TNF-RI. To date, nearly all functionally characterized adaptor proteins bind to the death domain of the TNF-RI receptor (3, 4). One protein, factor associated with neutral sphingomyelinase (nSMase) activity (FAN, also named NSMAF), binds to the more membrane-proximal nSMase activation domain (5). FAN belongs to the family of beige and Chediak-Higashi (BEACH) proteins. FAN is the smallest member of the BEACH protein family usually consisting of very large proteins with >2000-aa residues. Human FAN consists of 917 aa (amino acid), and FAN mRNA is expressed ubiquitously. At the C-terminal part, FAN contains five WD repeats that constitutively interact with the nSMase activation domain of TNF-RI (5). The N-terminal part of FAN contains a pleckstrin homology (PH) and a BEACH domain. FAN is mainly located at the plasma membrane, which is due to an interaction of the PH domain with 4,5-bis-phosphate (6). Biochemical studies and structural analysis suggested that the PH and BEACH domains interact to function as a single unit, which is essential for the activation of nSMase (7).

FAN has been implicated in TNF- and CD40-mediated induction of apoptosis (8, 9), lysosomal permeabilization (10), IL-6 secretion (11), interaction with the WD protein RACK1 (12), and regulation of cardiac cell death (13). Peppelenbosch et al. (14) suggested the involvement of the membrane-proximal region of TNF-RI in TNF-induced actin polymerization. We have previously reported that mouse embryonic fibroblasts (MEFs) isolated from FAN$^{-/-}$ mice were impaired in TNF-induced actin reorganization. Mechanistically, FAN connects the plasma membrane with the cytoskeleton and mediates TNF-induced Cdc42 activation and actin reorganization. Furthermore, FAN$^{-/-}$ MEFs are impaired in their motility in response to TNF in vitro, suggesting a role of FAN in cellular motility (6). To investigate the impact of FAN on immune cell migration and motility, we performed live imaging studies in zebrafish embryos. The zebrafish, *Danio rerio*, is emerging as a powerful model organism; it is both genetically

*Institute for Medical Microbiology, Immunology, and Hygiene, University of Cologne, 50935 Cologne, Germany; [†]European Molecular Biology Laboratory Heidelberg, 69117 Heidelberg, Germany; [‡]Institute for Biochemistry II, 50931 Cologne, Germany; [§]Center for Molecular Medicine Cologne, University of Cologne, 50935 Cologne, Germany; and [¶]Cologne Excellence Cluster on Cellular Stress Responses in Aging-Associated Diseases, University of Cologne, 50935 Cologne, Germany

[1]A.B. and D.S. contributed equally.

Address correspondence and reprint requests to Dr. Martin Krönke, Institute for Medical Microbiology, Immunology, and Hygiene, University of Cologne, Goldenfelsstrasse 19-21, D-50935 Köln, Germany. E-mail address: m.kroenke@uni-koeln.de

The online version of this article contains supplemental material.

Abbreviations used in this article: BEACH, beige and Chediak-Higashi; dpf, days postfertilization; FAN, factor associated with neutral sphingomyelinase activity; MEF, mouse embryonic fibroblast; MO, morpholino oligonucleotide; nSMase, neutral sphingomyelinase; PBST, PBS Tween-20; PH, pleckstrin homology; SMase, sphingomyelinase.

tractable and, translucent in larval stages, making it amenable to live-imaging approaches. We used zebrafish embryos to image the wound- and infection-triggered inflammatory response. The data obtained showed that leukocyte motility is impaired after knockdown of FAN in zebrafish, although the total numbers of leukocytes in the organism are not altered. The wound inflammatory response is dramatically disrupted by perturbing the mechanism by which leukocytes orient toward wound signals.

Materials and Methods

Characterization of FAN in zebrafish

The genomic database ensemble (htttp://www.ensembl.org/Danio_rerio/index) was searched for FAN homologs. One potential FAN homolog was identified (transcript ID ENSDART00000073635). This was used to determine the full-length sequence for the zebrafish FAN (Supplemental Fig. 1).

Sequence alignments of FAN from different species were made using Vector NTI (Invitrogen).

Morpholino-oligonucleotide injections

Antisense morpholino-modified oligonucleotides against zebrafish FAN were targeted against the splice sites of the second intron (FAN-E2I2, 5′-GTAAGCTGCTCACCTGTTTGTCTCG-3′; FAN-I2E2, 5′-GCCATTGGT-TCGCCTGTGTACAAAA-3′), and a standard control morpholino (5′-CC-TCTTACCTCAGTTACAATTTATA-3′) was obtained from Gene Tools. The injection solution consisted of 0.3 mM of each morpholino, 0.2% Phenol Red, and 0.1 M KCl, of which, on average, 2 nl was injected per embryo. Injection was performed by using an Eppendorf Femtojet and micromanipulator.

RNA isolation and RT-PCR

RNA from zebrafish embryos was isolated from embryos at different stages of development using the μMACS mRNA isolation kit (Miltenyi Biotec), according to the manufacturer's protocol, by addition of a DNase I digest for 7 min to remove traces of genomic DNA. First-strand synthesis was performed by utilizing the Superscript III system (Invitrogen) using 300 ng mRNA and random hexamer primers. For RT-PCR, 7.5 ng first-strand synthesis and RedTaq DNA polymerase (Sigma-Aldrich) were used. RT-PCR was performed as follows: 2 min at 94°C; 15 (β-actin) and 30 (FAN) cycles of 94°C for 15 s, 55°C for 30 s, 72°C for 1 min; 7 min at 72°C. For the amplification of FAN, the primers Fan-for1, 5′- ATGGCTTTCATCAC-GAAGAAG-3′ and Fan-rev1, 5′-CTAATACTATGGTTTCCACA-3′ were used. For the amplification of β-actin, the primers β-actin-for, 5′-ATG-GATGATGAAATTGCCGCAC-3′ and β-actin-rev, 5′-ACCATCACCA-GAGTCCATCACG-3′ were used.

Whole-mount in situ hybridization

Whole-mount in situ hybridization was performed, as described previously (15), with the only difference being that for this study no automated system was used.

Tail fin injury and confocal microscopy

The 2-days postfertilization (dpf) tg(PU1-Gal4-UAS-GFP; MPX-GFP; PU1-Gal4-UAS-RFP) (16, 17) embryos either injected with control MO or FAN-MO were anesthetized using tricaine (Sigma-Aldrich), according to standard protocols (18), to prevent embryos from twitching. Embryos were embedded laterally in a small drop of 1.2% low-melting agarose (Sigma-Aldrich) in a glass-bottom culture dish (MatTek) for wounding of the fin and subsequent microscopy. Wounds at the end of the tail fin were made using a pulsed 532-nm cutting laser. Images were taken directly before injury and 1.5 h after injury using an Olympus FV1000 confocal microscope and a ×40 water objective. Leukocytes that reached a defined area after 1.5 h were counted and statistically analyzed. For time-lapse microscopy, Z-series were collected at 2.30-min and 4-min intervals for 3.15 h. Projections of summed z stacks, time-lapse animation, and cell tracking were generated using Imaris (Bitplane).

To analyze leukocyte recruitment to the tail-fin wound, each cell was tracked (using Imaris) from the point when it appeared until the end of the time-lapse series, or, in case of the FAN-MO–injected embryos, until it disappeared again. The average speed of leukocytes and their straightness, which means the ratio of netto length and the total length, were analyzed by using Imaris. The straightness is a coefficient between 0 and 1. A higher straightness indicates a more directed migration toward the wound.

The morphology of cells during their migratory route was captured from individual frames of time-lapse movies using Image J, and tracing profiles

were color coded. These profiles outlined the protrusions extended by the cell and subsequently were analyzed whether a cell had made the right or the wrong choice of pseudopodia. A right choice of pseudopodia means that this pseudopodium is extended in the direction of movement. A wrong choice means that a pseudopodium is extended against the direction of movement. This analysis was performed for 10 morphant and 10 control cells.

Sudan black staining

The 2-dpf tg(PU1-Gal4-UAS-GFP) embryos either injected with FAN-MO or left untreated were injured with a scalpel and fixed 2 h postinjury in 4% paraformaldehyde for 2 h at room temperature. Embryos were washed three times with PBS Tween-20 (PBST). Next, embryos were incubated in 35% ethanol/65% PBST and 70% ethanol, each for 5 min. Afterward, embryos were transferred to a 0.18% Sudan black staining solution (Sigma-Aldrich 380B) and incubated for 20 min, followed by two short washing steps in 70% ethanol before they were progressively rehydrated. Subsequently, PBST was replaced by a 30% glycerol solution. This step was repeated with a 60 and 90% glycerol solution.

For analysis of the Sudan black staining, the embryos were transferred in 90% glycerol solution on a hollow grinding slide and brought into a suitable position using a fine needle. The embryos were then analyzed using a stereomicroscope (SMZ1500; Nikon) and photographed with a digital camera (DSFI1; Nikon).

Bacterial infection of the otic placode

Escherichia coli (DH5α) carrying the dsRed-expressing pGEMDs3 plasmid (19, 20) were grown in standard Luria-Bertani medium containing ampicillin (50 μg/ml). For infections, a 3-ml overnight culture was centrifuged for 3 min at 4000 × g, supernatant was removed, and the pellet was washed three times with PBS. After washing, the pellet was resuspended in 500 μl PBS. The final injection solution contained the washed E. coli diluted in PBS containing 1/10 Phenol Red.

The 2-dpf tg(PU1-Gal4-UAS-GFP) embryos injected with either a control MO or FAN-MO were anesthetized using tricaine (Sigma-Aldrich) and arranged on agarose plates for infection. Infection was achieved by injecting the bacteria into the otic placode by using an Eppendorf Femtojet and micromanipulator. Postinfection embryos were embedded laterally in a small drop of 1.2% low-melting agarose (Sigma-Aldrich) in a glass-bottom culture dish (MatTek). Confocal microscopy was performed by using an Olympus FV1000 confocal microscope and a ×40 water objective. Images were taken 30 min postinfection. Leukocytes that reached the side of infection after 30 min were counted and statistically analyzed.

Statistical analysis

Results were expressed as mean ± SEM. Statistical analysis was standard two-tailed Student t test for two data sets using Prism (GraphPad). The p values <0.05 (*), <0.01 (**), and <0.001 (***) were deemed as significant, highly significant, and most significant, respectively.

Results

Identification of zebrafish FAN

FAN is involved in TNF-mediated actin reorganization (6) and leukocyte recruitment (21). To test the function of FAN for leukocyte motility in vivo, we used the zebrafish (*Danio rerio*) as a model organism. The zebrafish embryo/larvae turned out to be a powerful model system to observe macrophage function in vivo (22–24). From this end, we first aimed to identify a FAN homolog in zebrafish. Zebrafish genome analysis revealed 5′ and 3′ parts of a single FAN homolog located on chromosome 7. FAN-specific PCR primer was designed, and the full-length gene was amplified from cDNA generated from zebrafish embryos 2 dpf. The zebrafish FAN gene encodes a protein with 911 aa and shows the typical signature of three functional domains, as follows: a weakly conserved PH domain (aa 191–286), a BEACH domain (aa 302–575), and five WD40 domains at the C terminus (aa 625–911) (Fig. 1A). Sequence comparison between mouse and zebrafish FAN revealed a total homology of 70% and a consensus homology of 78.5% (Supplemental Fig. 1). This high degree of conservation of FAN is observed in the entire animal kingdom, suggesting its evolutionary conserved role in cellular processes. RT-PCR analysis during early developmental stages revealed that FAN is expressed throughout
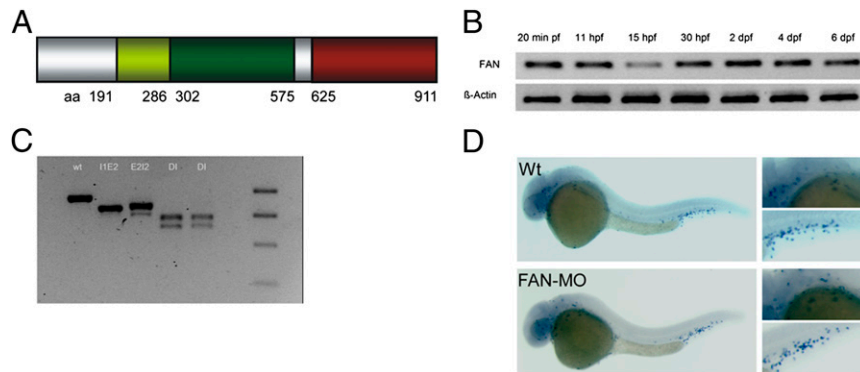
FIGURE 1. (**A**) Schematic drawing of the primary structure of zebrafish FAN. The PH, BEACH, and WD40 domains are shown in yellow, dark green, and red, respectively. (**B**) RT-PCR analysis of FAN during the early stages of development. mRNA was isolated from embryos at the indicated time points; β-actin was used as a positive control. FAN mRNA is already maternally provided and strongly expressed during the first 6 d of development. (**C**) RT-PCR to monitor the effect of the injected FAN antisense morpholinos. Injection of the single morpholinos (I1E2, E2I2) and combined injection (DI) abolishes the wild-type transcript. The combined injection of both morpholinos leads to the generation of two shorter splice variants. Sequence analysis of the two generated transcripts revealed a deletion of exons 2 and 3 and parts of exon 4 within the shorter transcript. Single injections were performed with a morpholino concentration of 0.3 mmol. Double injections were performed with a morpholino concentration of 0.3 mmol and 0.6 mmol. (**D**) Whole-mount in situ hybridization for *l*-plastin to visualize early leukocytes at 32 h postfertilization (hpf). For the in situ hybridization digoxygenin-labeled probes were used. The embryos were incubated with digoxygenin-labeled anti-sense RNA probes. The hybridized probes were detected immunochemically, by means of alkaline phosphatase-conjugated anti-digoxygenin Fab fragments, whereby the enzymatic conversion of specific substrates resulted in the production of colored precipitates. Small pictures on the *right side* are zoom-in areas for the head and the tail. No difference in number and distribution between wild-type and FAN knockdown embryos could be detected.

all analyzed stages of development until day 6 (Fig. 1B), which indicate a possible role of FAN during early developmental stages.

Influence of FAN propels leukocyte motility during wound response

To investigate the role of FAN in the migration of early leukocytes, the function of FAN was interfered with antisense morpholino oligonucleotides (MO) targeted against the splice sites of the second intron and were injected into one cell stage embryos. The injection of MOs generated two shorter splice variants, whereas the wild-type transcript could not be detected in injected embryos (Fig. 1C). Sequence analysis of the two generated transcripts revealed a deletion of exons 2 and 3 and parts of exon 4 within the shorter transcript. Both splice variants have a frameshift caused by the deletion of exons, resulting in a truncated protein.

To test whether the knockdown of FAN had any impact on total numbers of leukocytes in FAN morphants, in situ hybridization was performed using a probe against L-plastin, a marker for early leukocytes in zebrafish. In situ hybridization reveals that FAN morphant and control embryos have the same number of *l*-plastin–positive cells (Fig. 1D).

To investigate the influence of FAN on leukocyte motility, we injected either FAN-specific MOs or a control MO into one cell stage embryos and compared their wound inflammatory response at 2 dpf. For further experiments, the PU1-Gal4-UAS-GFP zebrafish line was used, which expresses GFP in leukocytes, allowing their observation in vivo (16). The 2-dpf embryos were injured with a cutting laser at the end of the tail fin, and the leukocytes that had reached the area indicated by the dashed line (Fig. 2A) were counted after 1.5 h. The number of leukocytes that reached the wound 1.5 h after injury was significantly reduced in FAN-MO–injected embryos compared with control embryos. On average only 1.9 ± 0.32 leukocytes reached the wound in FAN-MO–injected embryos, whereas 4.3 ± 0.39 and 4.7 ± 0.22 leukocytes were counted in the MO control and in wild-type embryos, respectively (Fig. 2B).

To reveal whether the reduced number of leukocytes at the site of injury affects the recruitment of both macrophages and neu-

trophils, we compared in a new set of experiments the total number of leukocytes labeled in the PU1-Gal4-UAS-GFP line with the number of neutrophils responding to injury. To achieve this, neutrophils were visualized by Sudan black staining in PU1-Gal4-UAS-GFP transgenic fish. Again, the total number of leukocytes recruited to the wounds was reduced in morphant embryos compared with control embryos. In control embryos on average 4.5 ± 0.34 leukocytes reach the site of injury, whereas in morphant embryos only 3 ± 0.35 leukocytes reach the site of injury. The number of neutrophils in morphants was reduced to 0.7 ± 0.17 compared with 1.6 ± 0.34 in control embryos (Fig. 2C–E). To determine the average number of macrophages, the number of neutrophils was subtracted from the total number of leukocytes. This shows a recruitment of 2.9 macrophages in control embryos compared with 2.3 macrophages in morphant embryos. In summary, the number of both macrophages and neutrophils is reduced in FAN-MO embryos. However, there is a stronger reduction in neutrophil recruitment than in macrophage recruitment (Fig. 2C), which is in line with the observations made by Montfort et al. (21).

In another set of experiments, a double-transgenic line (PU1-Gal4-UAS-RFP; MPX-GFP) was used to observe the number of leukocytes recruited to the wound. The total number of leukocytes is marked by PU1-Gal4-UAS-RFP (25), whereas neutrophils are marked with MPX-GFP (17). In this experiment, 11 leukocytes and 7.25 neutrophils are recruited to the wound in control embryos, and only 2 leukocytes and 1.5 neutrophils are recruited in FAN-MO embryos. This independent line of evidence confirms that the number of both macrophages and neutrophils that were recruited to the wound was reduced in FAN morphant embryos (Fig. 2F). The different numbers of leukocytes that were recruited to the side of injury in the two experiments are due to experimental setup. The embryos stained with Sudan black were counted under a binocular with lower magnification (11×1.6) because the Sudan black staining cannot be visualized with the confocal microscope. The double-transgenic line could be analyzed by confocal microscopy, which has a greater sensitivity partly due to z-stack technology.
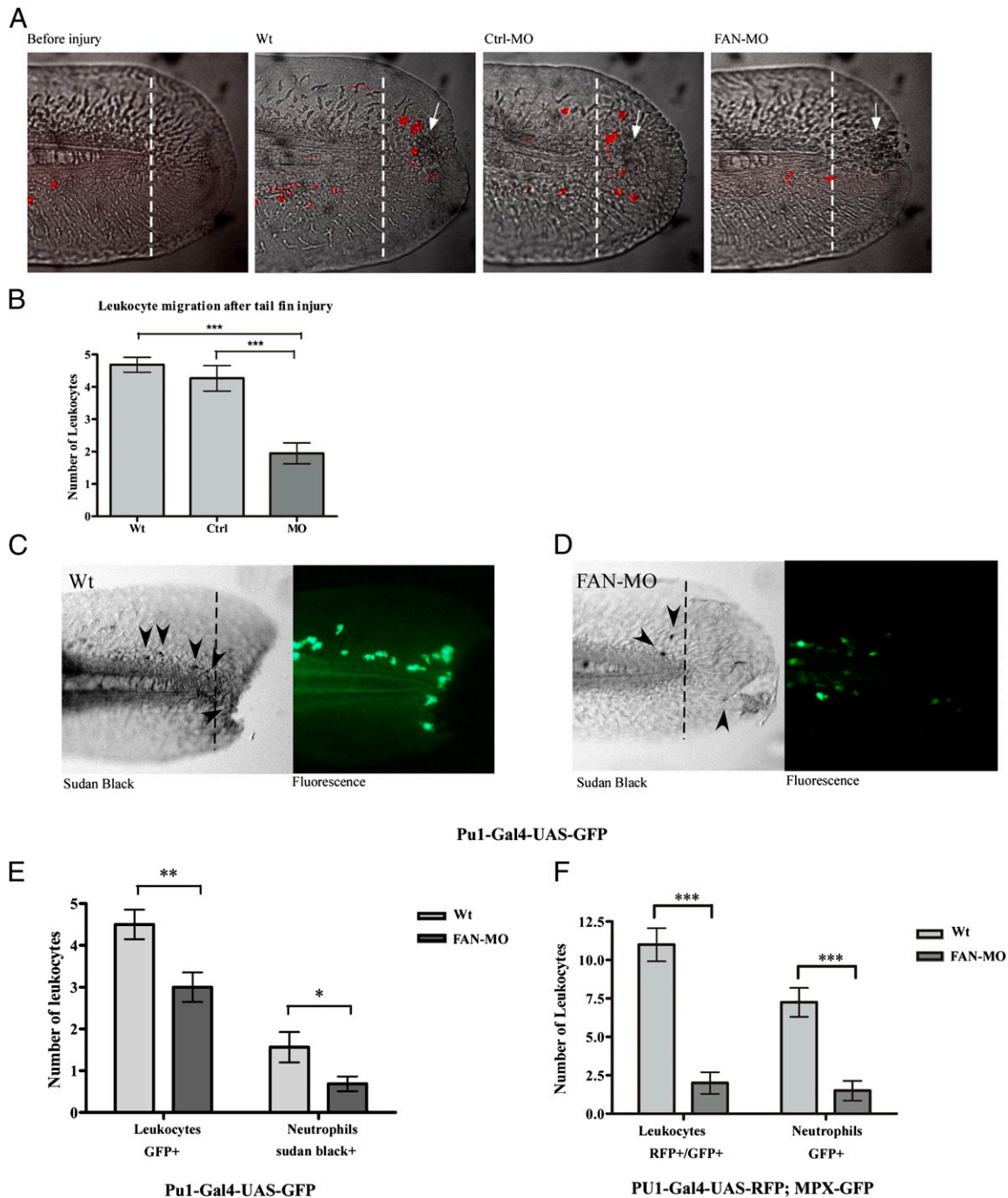
FIGURE 2. (**A**) Tail fin of a zebrafish embryo before laser injury. Wild-type, control, and FAN-MO–injected embryo 1.5 h after laser injury. The white arrow indicates the position of injury. The dashed line indicates the area in which leukocytes were counted after 1.5 h. (**B**) Statistical illustration of the number of leukocytes recruited to wild-type, control, and morphant wounds (Wt, $n = 19$, Ctrl, $n = 20$, MO, $n = 35$; ***p value Wt/MO <0.000004, ***p value Ctrl/MO <0.00005). (**C** and **D**) Sudan black staining and fluorescence analysis in Pu1-GAL4-UAS-GFP embryos. Embryos were injured with a scalpel. Embryos were fixed 2 h after tail fin injury. Green cells represent the total number of leukocytes that were recruited to the wound; neutrophils were stained with Sudan black (arrowheads). (**E**) Statistical illustration of the total number of leukocytes and the number of neutrophils recruited to control and morphant wounds after Sudan black staining and fluorescence analysis (Ctrl, $n = 16$, MO, $n = 15$; **p value Ctrl/MO [Pu1] <0.005, *p value Ctrl/MO [Sudan black] <0.03). (**F**) Statistical illustration of the total number of leukocytes and the number of neutrophils recruited to control and morphant wounds in double-transgenic embryos (PU1-Gal4-UAS-RFP; MPX-GFP) (Ctrl, $n = 5$, MO, $n = 5$; ***p value Ctrl/MO [PU1] <0.001, ***p value Ctrl/MO [MPX] <0.001).

FAN is required for oriented migration of leukocytes

The observed migration defect that results in fewer leukocytes reaching the side of injury might be due to a slower movement of leukocytes. Alternatively, the FAN knockdown might lead to a defect in the chemotactic migratory response, and therefore results in less leukocytes at the site of the wound. To further characterize the motility defect in FAN-MO–injected embryos and

to determine whether this is secondary to a reduced velocity of leukocytes or to a defect in chemotactic migratory response, time-course series for 3 h after injury were performed and the movement of leukocytes was tracked. Speed analysis of the leukocytes showed that the overall speed of leukocytes in FAN-MO–injected embryos does not significantly differ from that in control and wild-type embryos (Fig. 3B). Thus, the lower number of leuko-
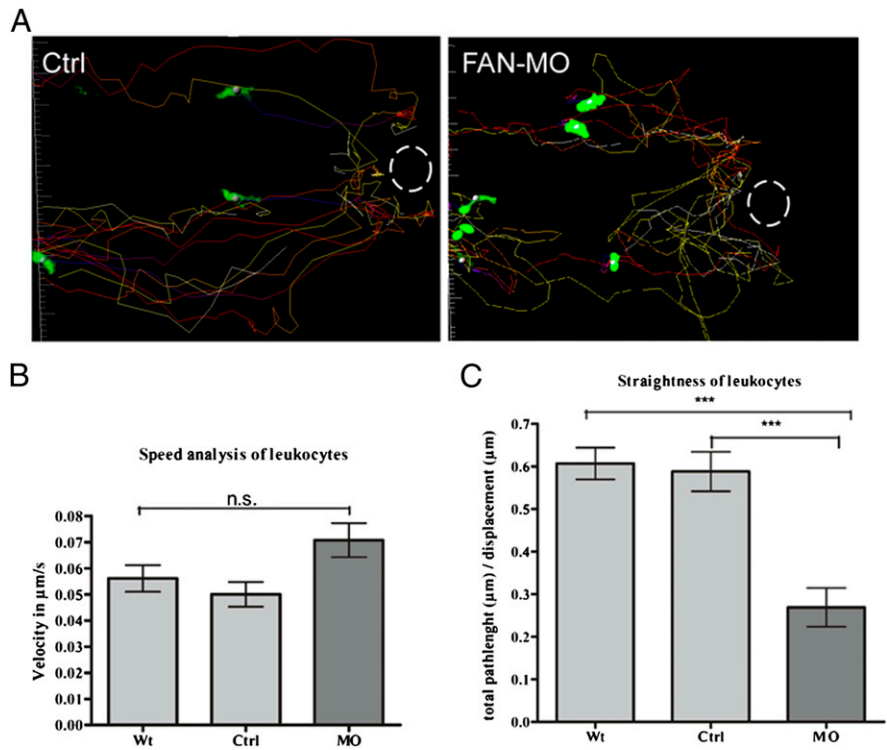
FIGURE 3. (**A**) Cell tracking from fluorescence movies up to 3 h after injury at the tail fin from 2-dpf embryos treated with control morpholino or FAN morpholino. A transgenic fishline (PU1-Gal4 UAS-GFP) was used for our experiments that has green fluorescent leukocytes. ×40 water objective. (**B**) Statistical illustration of the speed of leukocytes recruited to wounds in wild-type, control, and morphant embryos (Wt, $n = 18$, Ctrl, $n = 18$, MO, $n = 26$; p value Wt/MO <0.1 n.s., *p value Ctrl/MO <0.02). (**C**) Statistical illustration of the straightness of leukocytes recruited to wounds in wild-type, control, and morphant embryos (Wt, $n = 18$, Ctrl, $n = 18$, MO, $n = 26$; ***p value Wt/MO <0.000003, ***p value Ctrl/MO <0.00002).

cytes that reaches the wound after 1.5 h (Fig. 2A, 2B) is not due to a reduction of velocity.

Because the speed of leukocytes in FAN knockdown embryos and siblings was comparable, we analyzed the movement of leukocytes in greater detail. The number of leukocytes that move toward the wound in control embryos is larger than that in FAN-MO–injected embryos. Tracking of the leukocytes revealed that in control embryos leukocytes move straight toward the wound and
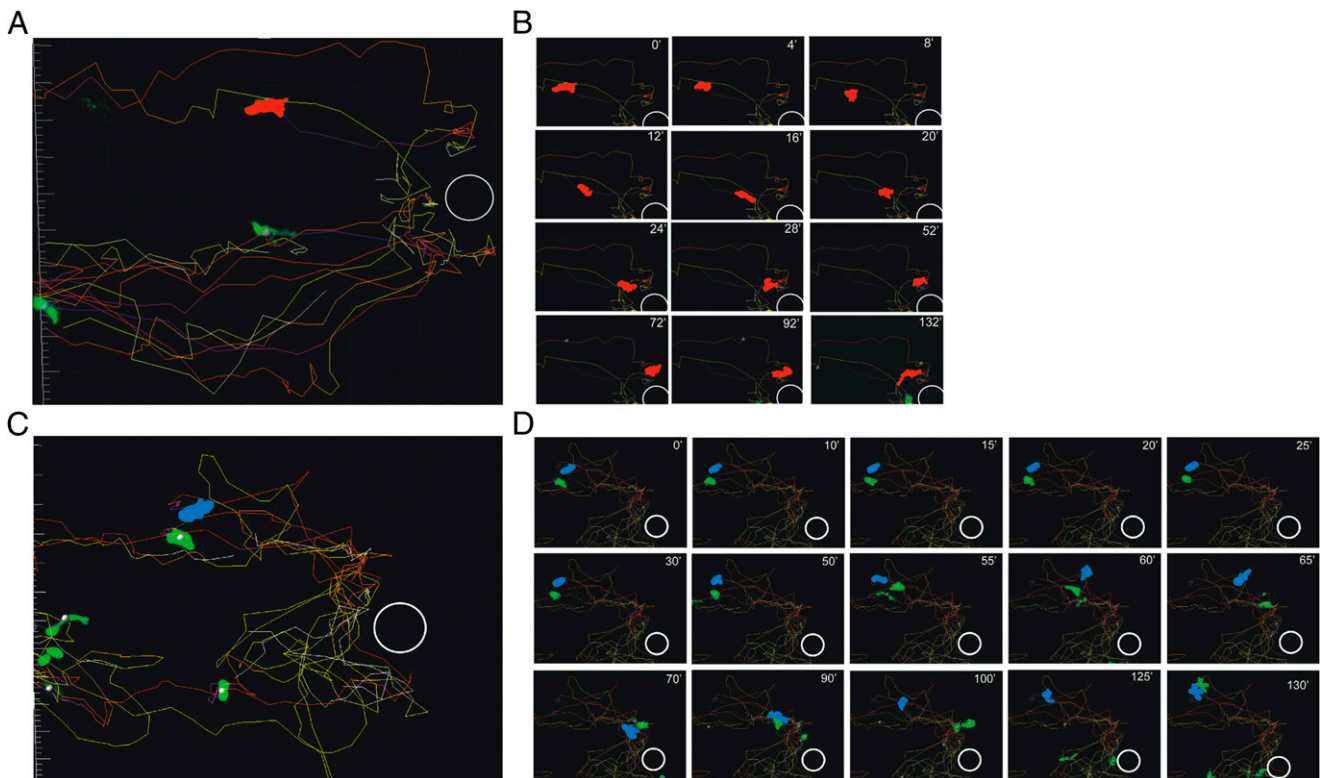

FIGURE 4. (**A**) Overview of cell tracking of a wild-type embryo. The white circle indicates the site of injury. (**B**) Detailed cell tracking of one leukocyte. The macrophage moves directly toward the wound and reaches it after 24 min. After reaching the wound, it stays there and does not move away from it. (**C**) Overview of cell tracking of a FAN morphant embryo. The white circle indicates the site of injury. (**D**) Detailed cell tracking of one leukocyte. The leukocyte does not move directly toward the wound, but performs protrusions in every direction before starting to move after 55 min. After 70 min, the macrophage reaches the wound, but directly starts to move away again. Single leukocytes were manually colored in red and blue by using ImageJ software. ×40 water objective.

remain there after reaching it (Figs. 3A, 4A, 4B, Supplemental Video 1). In contrast, in FAN-MO–injected embryos, leukocytes do not start directly to move toward the wound; they extend protrusions in every direction before they start to move toward the wound. Furthermore, they do not move directly toward the site of injury, but rather move in another direction, ending up in a circular movement, never reaching the wound (Figs. 3A, 4C, 4D, Supplemental Video 2). In addition, FAN-MO leukocytes that reach the wound often leave it again, and some leukocytes stop on their way to the wound, turn around, and disappear again, which was never observed in control embryos (Fig. 3A, Supplemental Videos 1 and 2). To measure this movement of the leukocytes toward the wound, we calculated the straightness, which is the quotient of the total path length divided by the displacement (netto length) of a tracked leukocyte. Investigation of the straightness revealed a significant difference between FAN-MO–injected embryos and wild-type and control embryos (Fig. 3C). In control and wild-type embryos, the straightness of leukocyte movement is 0.59 ± 0.05 and 0.61 ± 0.04, whereas in FAN-MO–injected embryos it is reduced to 0.27 ± 0.04. This reduction results in fewer numbers of leukocytes at the site of injury after 1.5 h in FAN knockdown embryos.

Notably, the morphology of migrating leukocytes in FAN morphant embryos appears different from that of control embryos. In control embryos, leukocytes have the typical shape with several pseudopodia from their leading edge and a retracting part without pseudopodia (Fig. 5A). In FAN morphant embryos, leukocytes often do not have a clear leading edge and they extend pseudo-
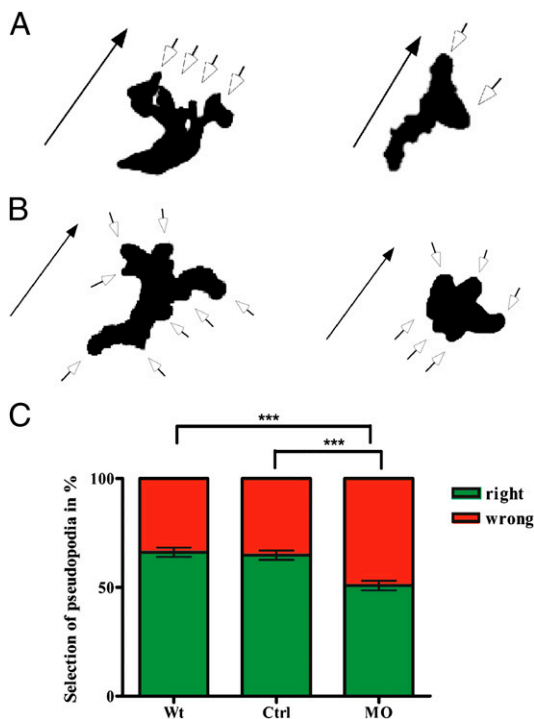
podia in all directions (Fig. 5B). They retract these pseudopodia and then extend new pseudopodia in other directions without moving (Supplemental Fig. 2). In addition, leukocytes in FAN knockdown embryos have more pseudopodia compared with control embryos (74 per leukocyte versus 33 in control embryos), and these cells more frequently made the wrong choice of pseudopodia (50.8% versus 66.1% correct turns in control embryos) (Fig. 5C).

Taken together, to our knowledge, we describe for the first time in vivo the role of FAN in leukocyte motility. Leukocytes of FAN knockdown embryos do not move slower than their siblings in wild-type embryos, but have a reduced straightness, exhibit an abnormal shape with more pseudopodia in the wrong direction, and thus reach the site of injury less efficiently. These findings are in line with our previous observations in cultured FAN-deficient MEFs showing altered cell polarity in a wound-scratch test upon TNF treatment (6).

Leukocyte migration upon infection in FAN knockdown embryos

To test whether the difference in leukocyte migration is tissue or stimulus dependent, the otic placode of 2-dpf embryos was infected with red fluorescent *E. coli* and the numbers of leukocytes reaching the site of infection was counted 30 min postinfection (Fig. 6A–C). Statistical analysis demonstrates that in this infection model the number of leukocytes that reach the site of infection is significantly reduced in FAN morphant leukocytes. In control embryos, on average 15.25 ± 1.9 leukocytes reach the site of
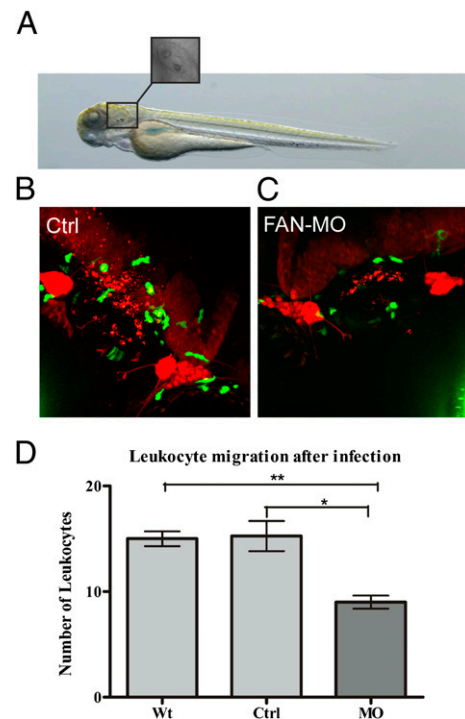

FIGURE 5. (**A**) A typical shape of control leukocytes. Leukocytes have one clear leading edge and a retracting part without pseudopodia. Arrow indicates the direction of move. Arrowheads indicate pseudopodia. (**B**) A typical shape of morphant leukocytes. Leukocytes extend pseudopodia in all directions without having a clear leading edge. Arrow indicates the direction of move. Arrowheads indicate pseudopodia. (**C**) Graphic illustration of the proportion of right choices (green) versus wrong choices (red) of pseudopodia made by control and wild-type versus morphant leukocytes (number of leukocytes: Wt, $n = 10$, Ctrl, $= 10$, MO, $= 10$; ***p value Wt/MO <0.0002, ***p value Ctrl/MO <0.0004).

FIGURE 6. (**A**) 3-dpf zebrafish larvae. The black rectangle marks the optic tectum, which is shown in a higher magnification (original magnification ×40) on top. (**B** and **C**) Fluorescent images of the optic tectum infected with dsRED-labeled *E. coli* in control (B) and FAN morphant embryos (C). (B) and (C) show the green fluorescent leukocytes of the transgenic fishline Pu1-Gal4 UAS-GFP and the dsRed-expressing *E. coli* injected into the otic placode. ×40 water objective. (**D**) Statistical illustration numbers of leukocytes recruited to wild-type, control, and morphant otic placodes postinfection with red fluorescent *E. coli* (Wt, $n = 5$, Ctrl, $n = 5$, MO, $n = 5$; **p value Wt/MO <0.003, *p value Ctrl/MO <0.01).

infection, whereas only 9 ± 0.85 leukocytes appear in FAN morphant embryos. This experiment provides evidence that the migration defect of leukocytes in morphant embryos is not tissue or stimulus dependent and implies a general role for FAN in the chemotactic migratory response.

Discussion

Evidence is accumulating suggesting that FAN might be involved in the motility of cells (6, 21). We recently reported that FAN links the TNF-RI to the actin cytoskeleton and is essentially involved in filopodia formation in MEF cells (6). Furthermore, recruitment of neutrophils into the peritoneal cavity was reduced by >50% in FAN-deficient mice (21). Although these findings suggest a role for FAN in cell motility, formal proof was missing. The use of a transgenic zebrafish line with fluorescently tagged leukocytes and the translucency of the embryos have now allowed us to demonstrate in vivo the essential role of FAN in the navigation of leukocytes toward chemotactic cues emanating from tissue damage or infection. Zebrafish larvae provide an ideal miniature model of the human wound migratory cell response, because only 20–30 leukocytes are drawn to a wound, and each of these cells can be tracked by live imaging with fine spatial and temporal precision.

We first identified a single FAN homolog in the zebrafish genome located on chromosome 7, which encodes for a protein with 911 aa and is expressed throughout all analyzed stages of development until day 6. Sequence comparison between mouse and zebrafish FAN revealed a total homology of 70% and a consensus homology of 78.5%, which suggests an evolutionary conserved role in cellular processes. FAN was successfully targeted by morpholinos injected into zebrafish embryos at the one- to two-cell stage. One important observation indicated that, upon injury at the tail fin, the number of leukocytes that assemble at the site of injury was markedly reduced in FAN-MO–injected embryos compared with wild-type or control embryos left untreated. Tracking of individual leukocytes revealed that reduced numbers of leukocytes arrive at the site of injury. This was due to an impaired directionality of leukocytes in FAN morphants. The average speed, however, was not affected.

The rapid recruitment of macrophages and neutrophils is essential to coordinate wound closure. Recently, Niethammer and coworkers (26) reported that a gradient of hydrogen peroxide is an initial chemoattractant generated by a wounded tail fin in zebrafish larvae. In fact, a myriad of signaling molecules originate from a wound such as chemokines that attract leukocytes to a wound site. Notably, TNF is released upon injury or infection and leukocytes start to move toward the site of TNF (19), suggesting that FAN action in chemotactic responses is triggered by TNF. This is consistent with our previous observation that FAN-deficient murine embryonic fibroblasts (MEFs) display an impaired Golgi apparatus reorientation in a scratch-wound test (6). This reorientation of the Golgi apparatus is independent of chemokines. In addition, isolated FAN-deficient MEFs show impaired migratory response to TNF (our unpublished data), suggesting that impaired TNF/FAN signaling is responsible for this defect. TNF is known to have a major function in the initiation and amplification of the inflammatory response by inducing the expression of chemotactic cytokines and chemokines that are responsible for the migration of several immune cells such as macrophages (27). There has been substantial recent progress in understanding how neutrophils develop and respond to inflammatory cues in zebrafish (17, 22, 23, 26, 28). Notably, FAN seems to be selectively involved in TNF-induced chemokine expression, including CXCL-2 and CCL-2, which are chemoattractants for neutrophils and macrophages, respectively (21). Thus, the possibility remains that

FAN morphants are unable to form an efficient chemoattractant gradient, which may contribute at least in part to decreased leukocyte recruitment to tail fin injury or to the infected otic placode.

To deal with the question how FAN might regulate the navigational capacity of leukocytes, it is instructive to consider the morphologic features of a cellular chemotactic response. Directional cues induce pseudopodia oriented toward the gradient, which includes selective retraction, oriented extension, and suppression of de novo pseudopodia formation (29). To move in the direction of a gradient, leukocytes must form many pseudopodia at the side of the cell that is facing the gradient. In this respect, it is important to note that leukocytes from FAN-deficient embryos protrude pseudopodia in all directions instead of having one clear leading edge. Leukocytes in FAN-deficient zebrafish larvae more often form pseudopodia at the wrong location, resulting in a loss of directionality. In addition, leukocytes from FAN-MO–injected embryos do not start directly to move toward the wound, which is probably also caused by multilateral protrusions observed before they start to move (Supplemental Video 2).

As to the molecular mechanisms regulating chemotaxis, studies in *Dictyostelium* have implicated many signaling pathways, including the phosphoinositide 3-kinase pathway activating AKT; the TorC2 pathway activating PKB1, a soluble guanylyl cyclase that is activated at the leading edge and produces cGMP; and phospholipase A_2, which has an unknown mechanism (30, 31). FAN signaling pathways may regulate pseudopodia formation in several ways. The observed defect in cell polarization and initiation of directed movement suggests problems in the cytoskeletal reorganization upon gradient sensing. The Rho family of small GTPases is known to play a central role in gradient sensing and cell polarization [reviewed by Charest and Firtel (32)]. Indeed, FAN mediates the TNF-induced modulation of the actin cytoskeleton through the small GTPase Cdc42 and VASP, which promotes F-actin bundling required for plasma membrane protrusions (6). We, therefore, assume that the loss of directionality in FAN knockdown leukocytes is due to impaired Cdc42 signaling. This is in line with the knockdown results of the Cdc42 effector molecule WASP. Cvejic et al. (22) could show that WASP knockdown macrophages have a reduced chemotactic index, resulting in a reduced number of macrophages reaching the site of injury.

Interestingly, FAN mediates the activation of nSMase by TNF (5, 33), which has been recently shown to involve the polycomb group protein EED (34). nSMase is a type C phospholipase-like phospholipase A_2 that plays a crucial role for pseudopodia splitting and directional migration in *Dictyostelium* (30, 31). Thus, it will be interesting to investigate whether FAN regulates the navigational capacity of leukocytes through neutral SMase.

It is important to note that we observed similar navigational defects postinfection of the otic placode with red fluorescent *E. coli*. The reaction of FAN-deficient leukocytes to infection was impaired so that they cannot move directly toward the site of infection. Moreover, FAN-deficient leukocytes seem to have lost their orientation. Similar defective migratory phenotypes of leukocytes in two different tissues with two different stimuli suggest that FAN plays a general role in chemotaxis.

Disclosures

The authors have no financial conflicts of interest.

References

1. Wiegmann, K., S. Schütze, E. Kampen, A. Himmler, T. Machleidt, and M. Krönke. 1992. Human 55-kDa receptor for tumor necrosis factor coupled to signal transduction cascades. *J. Biol. Chem.* 267: 17997–18001.
2. Hehlgans, T., and D. N. Männel. 2002. The TNF-TNF receptor system. *Biol. Chem.* 383: 1581–1585.
3. Wajant, H., K. Pfizenmaier, and P. Scheurich. 2003. Tumor necrosis factor signaling. *Cell Death Differ.* 10: 45–65.
4. Chen, G., and D. V. Goeddel. 2002. TNF-R1 signaling: a beautiful pathway. *Science* 296: 1634–1635.
5. Adam-Klages, S., D. Adam, K. Wiegmann, S. Struve, W. Kolanus, J. Schneider-Mergener, and M. Krönke. 1996. FAN, a novel WD-repeat protein, couples the p55 TNF-receptor to neutral sphingomyelinase. *Cell* 86: 937–947.
6. Haubert, D., N. Gharib, F. Rivero, K. Wiegmann, M. Hösel, M. Krönke, and H. Kashkar. 2007. PtdIns(4,5)P-restricted plasma membrane localization of FAN is involved in TNF-induced actin reorganization. *EMBO J.* 26: 3308–3321.
7. Jogl, G., Y. Shen, D. Gebauer, J. Li, K. Wiegmann, H. Kashkar, M. Krönke, and L. Tong. 2002. Crystal structure of the BEACH domain reveals an unusual fold and extensive association with a novel PH domain. *EMBO J.* 21: 4785–4795.
8. Ségui, B., N. Andrieu-Abadie, S. Adam-Klages, O. Meilhac, D. Kreder, V. Garcia, A. P. Bruno, J. P. Jaffrézou, R. Salvayre, M. Krönke, and T. Levade. 1999. CD40 signals apoptosis through FAN-regulated activation of the sphingomyelin-ceramide pathway. *J. Biol. Chem.* 274: 37251–37258.
9. Ségui, B., O. Cuvillier, S. Adam-Klages, V. Garcia, S. Malagarie-Cazenave, S. Lévêque, S. Caspar-Bauguil, J. Coudert, R. Salvayre, M. Krönke, and T. Levade. 2001. Involvement of FAN in TNF-induced apoptosis. *J. Clin. Invest.* 108: 143–151.
10. Werneburg, N., M. E. Guicciardi, X. M. Yin, and G. J. Gores. 2004. TNF-alpha-mediated lysosomal permeabilization is FAN and caspase 8/Bid dependent. *Am. J. Physiol. Gastrointest. Liver Physiol.* 287: G436–G443.
11. Malagarie-Cazenave, S., B. Ségui, S. Lévêque, V. Garcia, S. Carpentier, M. F. Altié, A. Brouchet, V. Gouazé, N. Andrieu-Abadie, Y. Barreira, et al. 2004. Role of FAN in tumor necrosis factor-alpha and lipopolysaccharide-induced interleukin-6 secretion and lethality in D-galactosamine-sensitized mice. *J. Biol. Chem.* 279: 18648–18655.
12. Tcherkasowa, A. E., S. Adam-Klages, M. L. Kruse, K. Wiegmann, S. Mathieu, W. Kolanus, M. Krönke, and D. Adam. 2002. Interaction with factor associated with neutral sphingomyelinase activation, a WD motif-containing protein, identifies receptor for activated C-kinase 1 as a novel component of the signaling pathways of the p55 TNF receptor. *J. Immunol.* 169: 5161–5170.
13. O'Brien, N. W., N. M. Gellings, M. Guo, S. B. Barlow, C. C. Glembotski, and R. A. Sabbadini. 2003. Factor associated with neutral sphingomyelinase activation and its role in cardiac cell death. *Circ. Res.* 92: 589–591.
14. Peppelenbosch, M., E. Boone, G. E. Jones, S. J. van Deventer, G. Haegeman, W. Fiers, J. Grooten, and A. J. Ridley. 1999. Multiple signal transduction pathways regulate TNF-induced actin reorganization in macrophages: inhibition of Cdc42-mediated filopodium formation by TNF. *J. Immunol.* 162: 837–845.
15. Sieger, D., D. Tautz, and M. Gajewski. 2003. The role of Suppressor of Hairless in Notch mediated signalling during zebrafish somitogenesis. *Mech. Dev.* 120: 1083–1094.
16. Peri, F., and C. Nüsslein-Volhard. 2008. Live imaging of neuronal degradation by microglia reveals a role for v0-ATPase a1 in phagosomal fusion in vivo. *Cell* 133: 916–927.
17. Renshaw, S. A., C. A. Loynes, D. M. Trushell, S. Elworthy, P. W. Ingham, and M. K. Whyte. 2006. A transgenic zebrafish model of neutrophilic inflammation. *Blood* 108: 3976–3978.
18. Westerfield, M. 1995. *The Zebrafish Book.* University of Oregon Press, Eugene, OR.
19. Sieger, D., C. Stein, D. Neifer, A. M. van der Sar, and M. Leptin. 2009. The role of gamma interferon in innate immunity in the zebrafish embryo. *Dis. Model Mech.* 2: 571–581.
20. van der Sar, A. M., R. J. Musters, F. J. van Eeden, B. J. Appelmelk, C. M. Vandenbroucke-Grauls, and W. Bitter. 2003. Zebrafish embryos as a model host for the real time analysis of *Salmonella typhimurium* infections. *Cell. Microbiol.* 5: 601–611.
21. Montfort, A., B. de Badts, V. Douin-Echinard, P. G. Martin, J. Iacovoni, C. Nevoit, N. Therville, V. Garcia, M. A. Bertrand, M. H. Bessières, et al. 2009. FAN stimulates TNF(alpha)-induced gene expression, leukocyte recruitment, and humoral response. *J. Immunol.* 183: 5369–5378.
22. Cvejic, A., C. Hall, M. Bak-Maier, M. V. Flores, P. Crosier, M. J. Redd, and P. Martin. 2008. Analysis of WASp function during the wound inflammatory response: live-imaging studies in zebrafish larvae. *J. Cell Sci.* 121: 3196–3206.
23. Feng, Y., C. Santoriello, M. Mione, A. Hurlstone, and P. Martin. 2010. Live imaging of innate immune cell sensing of transformed cells in zebrafish larvae: parallels between tumor initiation and wound inflammation. *PLoS Biol.* 8: e1000562.
24. Zhang, Y., X. T. Bai, K. Y. Zhu, Y. Jin, M. Deng, H. Y. Le, Y. F. Fu, Y. Chen, J. Zhu, A. T. Look, et al. 2008. In vivo interstitial migration of primitive macrophages mediated by JNK-matrix metalloproteinase 13 signaling in response to acute injury. *J. Immunol.* 181: 2155–2164.
25. Sieger, D., C. Moritz, T. Ziegenhals, S. Prykhozhij, and F. Peri. Long range Ca2+ waves transmit brain damage signals to microglia. *Dev. Cell*
26. Niethammer, P., C. Grabher, A. T. Look, and T. J. Mitchison. 2009. A tissue-scale gradient of hydrogen peroxide mediates rapid wound detection in zebrafish. *Nature* 459: 996–999.
27. Torrente, Y., E. El Fahime, N. J. Caron, R. Del Bo, M. Belicchi, F. Pisati, J. P. Tremblay, and N. Bresolin. 2003. Tumor necrosis factor-alpha (TNF-alpha) stimulates chemotactic response in mouse myogenic cells. *Cell Transplant.* 12: 91–100.
28. Mathias, J. R., B. J. Perrin, T. X. Liu, J. Kanki, A. T. Look, and A. Huttenlocher. 2006. Resolution of inflammation by retrograde chemotaxis of neutrophils in transgenic zebrafish. *J. Leukoc. Biol.* 80: 1281–1288.
29. Van Haastert, P. J. 2010. Chemotaxis: insights from the extending pseudopod. *J. Cell Sci.* 123: 3031–3037.
30. Bosgraaf, L., and P. J. Van Haastert. 2009a. Navigation of chemotactic cells by parallel signaling to pseudopod persistence and orientation. *PLoS One* 4: e6842.
31. Bosgraaf, L., and P. J. Van Haastert. 2009b. The ordered extension of pseudopodia by amoeboid cells in the absence of external cues. *PLoS One* 4: e5253.
32. Charest, P. G., and R. A. Firtel. 2007. Big roles for small GTPases in the control of directed cell movement. *Biochem. J.* 401: 377–390.
33. Adam, D., K. Wiegmann, S. Adam-Klages, A. Ruff, and M. Krönke. 1996. A novel cytoplasmic domain of the p55 tumor necrosis factor receptor initiates the neutral sphingomyelinase pathway. *J. Biol. Chem.* 271: 14617–14622.
34. Philipp, S., M. Puchert, S. Adam-Klages, V. Tchikov, S. Winoto-Morbach, S. Mathieu, A. Deerberg, L. Kolker, N. Marchesini, D. Kabelitz, et al. 2010. The Polycomb group protein EED couples TNF receptor 1 to neutral sphingomyelinase. *Proc. Natl. Acad. Sci. USA* 107: 1112–1117.